

CASE REPORT

Retinal hamartomas at different stages in a patient with tuberous sclerosis: A OCT-SS description

Paula Basso Dias  | Anna Carolina Badotti Linhares  | Kenzo Hokazono 

Department of Ophthalmology,
Universidade Federal do Paraná,
Curitiba, Brazil

Correspondence

Kenzo Hokazono, Department of
Ophthalmology, Universidade Federal
do Paraná, R. da Paz, 195 (123),
Curitiba – PR, 80060-160, Brazil.
Email: kenzo_hokazono@hotmail.com

Key Clinical Message

Retinal astrocytic hamartoma (RAH) is a benign glial tumor that may be present in patients with tuberous sclerosis (TS), contributing to the diagnosis of this syndrome. While hamartomas identified through indirect ophthalmoscopy are often large enough to affect vessels and optic disc anatomy, RAH not detected in previous fundoscopies may become apparent in optical coherence tomography (OCT). The purpose of this report was to describe and characterize RAH with OCT with swept-source technology (OCT-SS), aiming to establish a more comprehensive classification for these hamartomas due to their diverse presentations. Fundus examination of a 11-year-old girl revealed retinal tumors in both eyes. OCT-SS confirmed the diagnosis of TS, revealing dome-shaped hyperreflective masses at different stages of evolution. Lesion 1: maximum thickness (MT) of 336 μm and ganglion cell layer disorganization. Lesion 2: MT of 438 μm and preserved outer plexiform layer. Lesion 3: posterior shadow, MT of 1478 μm and complete rupture of retinal anatomy. Lesion 4: MT of 342 μm and preserved retinal anatomy. OCT is a noninvasive method which assists the diagnosis of subclinical lesions and clinical characterization of TS patients.

KEYWORDS

case report, OCT, optical coherence tomography, retinal hamartomas, tuberous sclerosis

1 | INTRODUCTION

Retinal astrocytic hamartoma (RAH) is a benign glial tumor that may be present in patients with tuberous sclerosis (TS),¹ a genetic phakomatosis caused by the mutation of the tumor suppressor genes TSC1 or TSC2, affecting ~1 in 6000 people.^{2–4} Although TS is typically identified by the Vogt triad (facial angiofibroma, mental retardation, and intractable epilepsy), less than 40% of affected

patients exhibit all three features, necessitating a careful ophthalmic examination.⁵

Ocular involvement in TS can manifest in several forms, such as hypopigmented iris spots, RAHs, and retinal pigment epithelial depigmentation spots. Among these, RAH is the most well-known, representing a benign intraocular tumor that appears as a yellow-gray mass, either sessile or slightly elevated, within the nerve fiber layer of the retina.⁵ In diagnosing TS, two major criteria or one major

Paula Basso Dias, Anna Carolina Badotti Linhares and Kenzo Hokazono are contributed equally to this study.

This is an open access article under the terms of the [Creative Commons Attribution-NonCommercial-NoDerivs](https://creativecommons.org/licenses/by-nc-nd/4.0/) License, which permits use and distribution in any medium, provided the original work is properly cited, the use is non-commercial and no modifications or adaptations are made.

© 2023 The Authors. *Clinical Case Reports* published by John Wiley & Sons Ltd.

and two minor criteria are required, with RAH being one of the major criteria.^{6,7}

Hamartomas identified through indirect ophthalmoscopy are often of a sufficient size to alter vessels and optic disc anatomy. However, RAHs that were not detected in previous fundoscopic examinations may become visible when using OCT. The use of OCT revealed the prevalence of RAH in 80% of patients with TS,⁶ which highlights the clinical relevance of a noninvasive diagnostic method of subclinical lesions and clinical characterization of patients with TS.⁶

OCT was originally introduced in 1991 and has since been employed for in vivo imaging of retina. The high speed and the long wavelength (~1050 nm) of OCT with swept-source technology (OCT-SS) offer significantly improved spatial resolution, a larger field of view, enhanced tissue penetration, and superior sensitivity roll-off performance. These attributes provide both detailed qualitative and quantitative information about the retinal structure and vasculature, proving to be fundamental for the diagnosis and monitoring of several diseases.⁴

In previous studies, the imaging features of RAH were described using time-domain OCT; however, the low resolution of this technique limited definitive descriptions of certain features.⁵ To overcome this limitation, our study used higher resolution OCT-SS, which enabled more detailed visualization of each tumor.

It was noted that hamartomas exhibit an initial involvement of the inner retina layers, and as they grow and calcify, they progress toward the outer layers. To enhance the classification of retinal hamartomas, further descriptive studies focusing on OCT aspects are essential, due to their high prevalence in patients with TS. The purpose of this report was to describe and characterize retinal hamartomas at different stages of evolution using OCT-SS of a patient with TS.

2 | CASE PRESENTATION

A 11-year-old female patient underwent a slit-lamp biomicroscopic examination that showed no abnormalities

in both eyes. However, during the fundus examination, bilateral retinal tumors were observed: six in the right eye (RE) (Figure 1) and five in the left eye (LE) (Figure 1B).

In the RE, there were two lesions located inferotemporally, two superotemporally, one inferonasally, and one superiorly. The inferotemporal lesion appeared yellow, elevated, with central calcification, and with a translucent area on the periphery, which is consistent with the typical description of transitional hamartomas, also known as type III astrocytic hamartomas. The other five lesions located at the arcade level displayed a yellow/gray-color, translucency, imprecise limits, no calcifications, and with obscuration of retinal vasculature. These features correspond to astrocytic type I hamartomas or flat hamartomas.

In the LE, all tumors were found at the arcade level, consisting of two lesions located superotemporally, one inferotemporally, and two in the temporal periphery. All these tumors were classified as type I astrocytic hamartomas. Neither eye showed any evidence of retinal detachment, lesions affecting the optic disc or involvement of the macula.

The OCT examination confirmed the diagnosis of TS, revealing dome-shaped hyperreflective masses in both eyes at different stages of evolution. In the RE, three different spectra of lesions were observed, all exhibiting a gradual transition to the normal retina.

Lesion 1, at an earlier stage, had a maximum thickness (MT) of 336 μm , with preserved inner nuclear and inner plexiform layers. However, there was disorganization of the ganglion cell layer (Figure 2). Lesion 2, with a MT of 438 μm , showed disruption in the normal structure of the retinal layers, and there was disorganization in the ganglion cell, inner nuclear, and inner plexiform layers, with the outer plexiform layer apparently preserved (Figure 2). However, the following OCT scan showed the hamartoma causing a compressive effect in the neurosensory retina with thinning of all retinal layers including the outer nuclear layer. A thickened inner nuclear layer can also be observed (Figure 3).

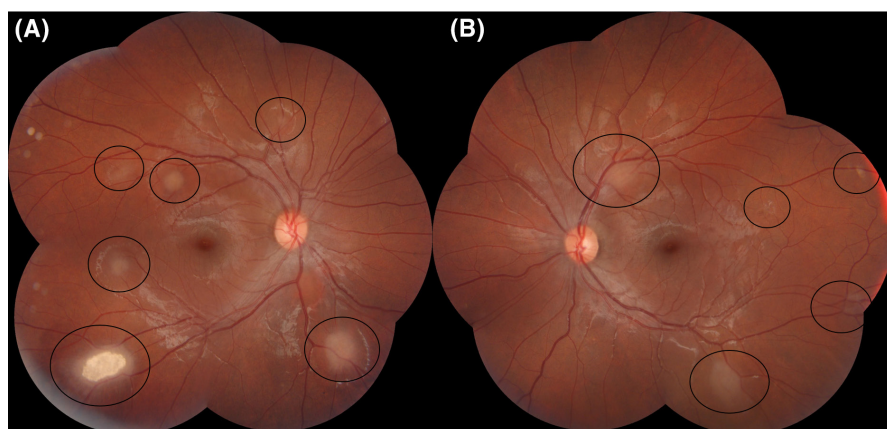
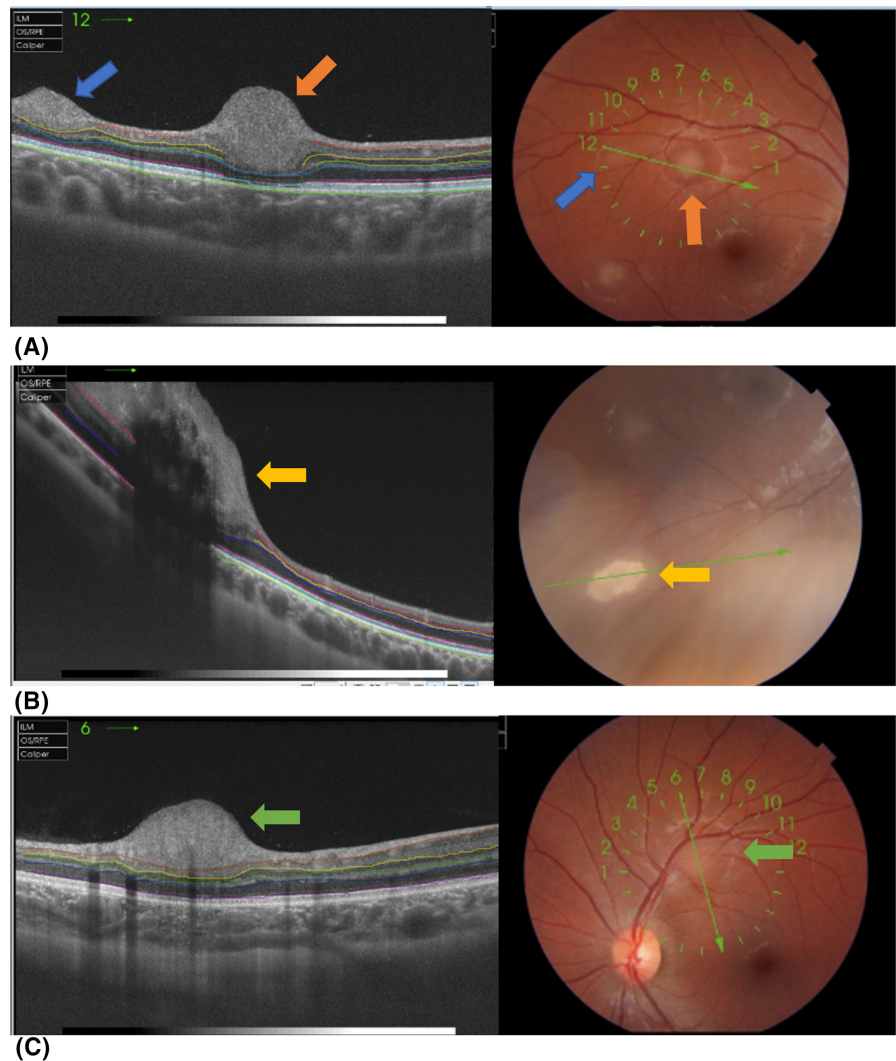


FIGURE 1 (A and B) Fundus photography showing six lesions in the right eye (A) and five in the left eye (B).

FIGURE 2 (A–C) OCT showing Lesion 1 (blue arrow), MT of 336 μm , preserved inner nuclear and inner plexiform layers and disorganization of the ganglion cell layer (A). Lesion 2 (orange arrow), MT of 438 μm , disruption in the normal structure of the retinal layers with disorganization of the ganglion cell, inner nuclear and inner plexiform layers (A). Lesion 3 (yellow arrow), a hyperreflective dome-shaped proliferation with posterior shadow, MT of 1478 μm , presented “moth-eaten” empty optical spaces, with an apparent complete rupture of the retinal anatomy (B). Lesion 4 (green arrow), MT of 342 μm , preserved the retinal anatomy, located at the level of the RNFL, making it possible to identify the ganglion cell layer (C).



Lesion 3, categorized as transitional, appeared as a hyperreflective dome-shaped proliferation with a posterior shadow. It had a MT of 1478 μm and showed “moth-eaten” empty optical spaces, with an apparent complete rupture of the retinal anatomy (Figure 2B). In the LE, Lesion 4 was observed with a MT of 342 μm preserving the retinal anatomy and located at the level of the retinal nerve fiber layer (RNFL), making it possible to identify the ganglion cell layer, different from Lesion 1 (Figure 2C). OCT scan also shows a retinal vessel inside the hamartoma, causing a shadow effect (Figure 4).

During the 1-year follow-up, the RAHs remained stable in the OCT examination, and the patient maintained a visual acuity of 1.0 in both eyes. She will continue follow-up with her ophthalmologist.

3 | DISCUSSION

The hamartomas present themselves in a heterogeneous way, which had led to their classification in three groups.

Type 1 hamartomas are relatively flat, translucent, gray-white lesions without calcifications. Type 2 hamartomas are elevated, multinodular, calcified, opaque and have a characteristic “blackberry” shaped. Finally, type 3 hamartomas represent transitional lesions, displaying features that combine characteristics of both type 1 and type 2 hamartomas. Type 1 injury has been described as the most common, occurring in up to 70% of cases, followed by type 2 (55%) and type 3 (9%).⁸ However, studies in different populations have shown variations in the prevalence of each type.^{7,8} For instance, Zhang et al. reported a higher prevalence of type 1 RAH (94%) in Chinese patients, while type 2 and type 3 were less common.⁷ Such discrepancies suggest that ethnicity may play a significant role in the development of RAHs.⁷ Furthermore, Zhan et al. showed that these lesions can coexist, as they found more than one type of RAH in 17.4% of TS patients.⁹

To further refine the classification of RAHs based on OCT findings, Pichi et al. proposed a new classification system, which includes: type I, a flat lesion within the RNFL without retinal traction; type II, a mildly elevated

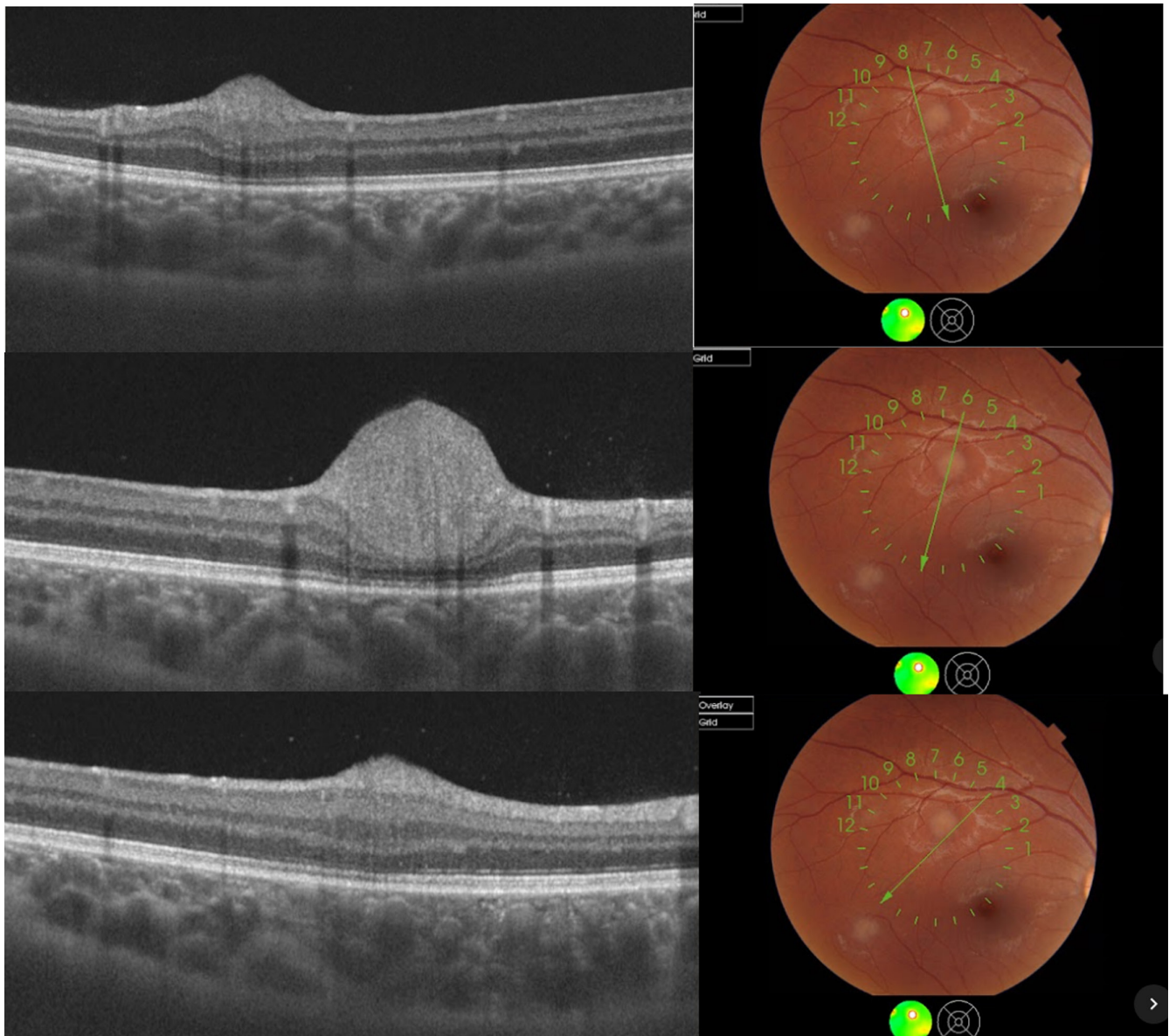


FIGURE 3 OCT scans and fundus photography showing Lesion 2. Top: the OCT scan passing in the temporal limit of the hamartoma. Note the inner retinal layers preserved and the irregular inner nuclear layer (red arrow). Middle: the hamartoma caused a compressive effect in the neurosensory retina with thinning of all retinal layers including the outer nuclear layer. Bottom: OCT scan passing in the nasal limit of the hamartoma. Note the thickened inner nuclear layer (red arrow).

hyperreflective lesion (height $< 500 \mu\text{m}$) with retinal traction and internal retinal disorganization; type III, an elevated retinal mass (height $> 500 \mu\text{m}$), mushroom shaped, with internal retinal calcification with “moth-eaten” appearance; and finally, type IV, an elevated (height $> 500 \mu\text{m}$) dome-shaped, non-calcified retinal mass with an optically empty cavity.⁵

Mutolo et al. introduced a new subcategory of hamartomas (type IIb), in addition to type IIa lesions, which were described by Pichi et al. as type II. Type IIb lesions are characterized by an elevated retinal mass ($> 500 \mu\text{m}$) above the RNFL with or without retinal adhesion or traction on the tumor surface. They are associated with

a intratumorally heterogeneous appearance, which may vary from a solid appearance to the presence of intralésional small empty spaces or cysts, and the presence of segmented vascular calcifications. The involvement of the inner retinal layer, outer retinal layer, and full retinal thickness may occur, with or without posterior optical shadowing.⁶

In our report, four different spectra of lesions were observed in the OCT. According to Pichi et al.,⁵ the lesions can be categorized as type I (lesion 4), type II—corresponding to type IIa in the Mutolo et al.⁶ classification—and type III (Lesions 2 and 3, respectively). However, one of the injuries did not fit this classification (Lesion 1). Lesion 1 exhibited

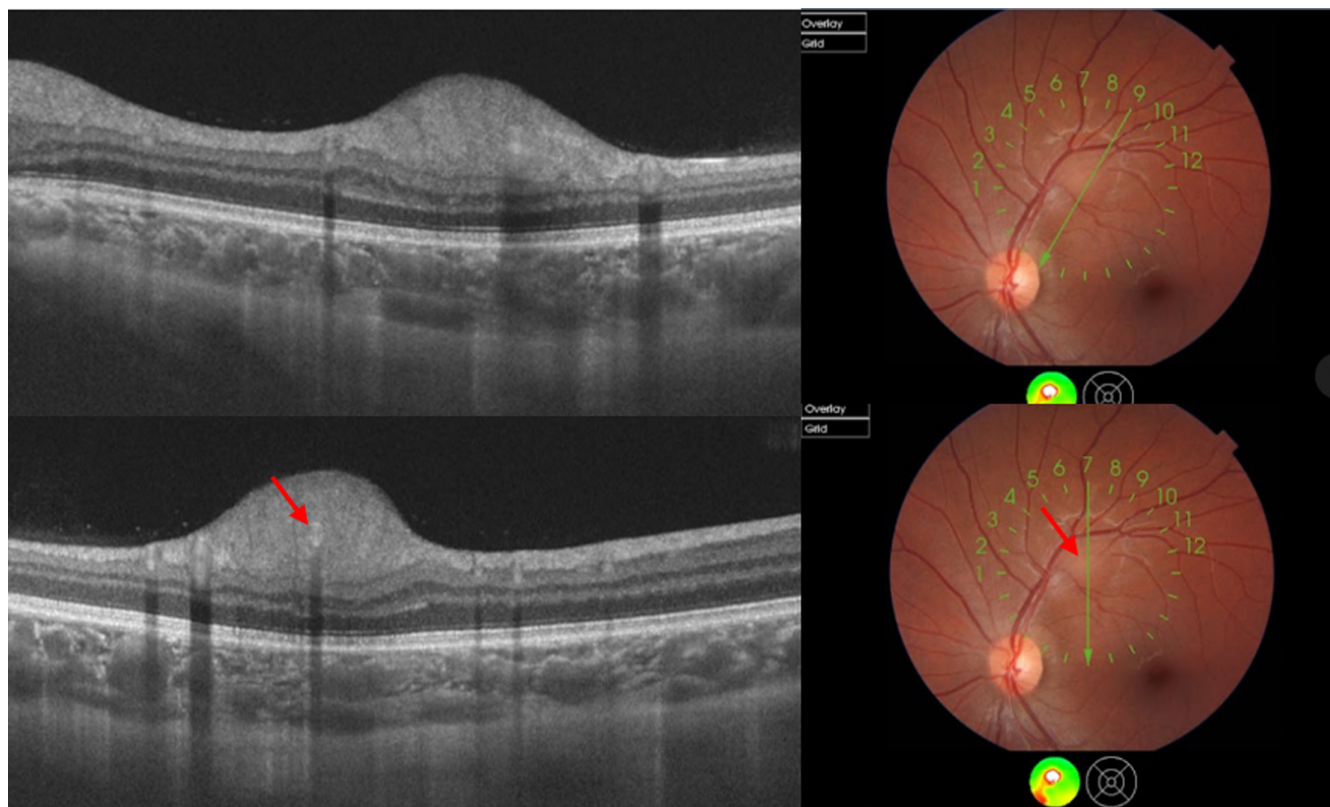


FIGURE 4 OCT scan and fundus photography of Lesion 4. Top: an initial lesion with preserved ganglion cell layer, inner plexiform layer, and inner nuclear layer. Bottom: the same initial lesion with retinal nerve fiber layer involvement. Note a retinal vessel inside the hamartoma (red arrow) causing a shadow effect in the OCT. The vessel is not visible in the fundus photography due to the lesion.

type IIa features, but had a MT of $<500\mu\text{m}$. Another challenge for classification was the involvement of the retinal layers. Even though Lesion 2 was classified as type IIa, it showed different involvement of the retinal layers compared to Lesion 1, which was also classified as type IIa. The difficulty found in classification has also been reported by Kato et al. and Mutolo et al., which reinforces the need for more descriptive studies of OCT aspects.^{6,10}

Zhang et al demonstrated that more than half of type 1 RAHs are located in the temporal retina, often near the end of the arcades.⁷ In our report, 66.6% of the lesions in the RE and 100% of the lesions in the LE were found in the temporal region. On the other hand, calcified RAHs, especially type 2, are more commonly found in the peripapillary region. This distribution pattern could be related to the observation of greater retinal vascular diameters in the temporal retina, indicating a higher blood supply compared to the nasal region, which may explain the higher incidence of RAHs in this the temporal area.^{9,11}

The use of OCT in demonstrating the microstructure of RAHs is not only useful for detecting small or semi-transparent lesions that might be easy to miss during examination, but also helps the differentiation of RAH from retinoblastoma, combined retinal hamartoma and choroidal tumors.^{1,8} Furthermore, some

authors have suggested that translucent tumors may evolve over time into multinodular lesions with cystic, hyaline or calcified changes, as if type 2 tumors represent a late stage of the lesions.¹² Therefore, OCT may also facilitate the follow-up of RAHs and aid in tracking their progression.^{6,12}

4 | CONCLUSION

This study utilized OCT-SS to describe four distinct spectra of hamartomas, providing a more comprehensive evaluation of these lesions. The observation that hamartomas initially affect the inner retinal layers and progress to the outer layers as they grow and calcify was highlighted. OCT proved to be a valuable noninvasive tool for diagnosing subclinical lesions and contributing to the clinical characterization of patients with TS. However, due to the heterogeneity of these lesions and their high prevalence in patients with TS, further descriptive studies focusing on OCT aspects are essential to achieve a better classification of retinal hamartomas. Such research will ultimately contribute to improving our understanding of these tumors and optimizing their diagnosis and management.

AUTHOR CONTRIBUTIONS

Paula Basso Dias: Conceptualization; data curation; formal analysis; investigation; methodology; project administration; resources; validation; visualization; writing – original draft; writing – review and editing. **Anna Carolina Badotti Linhares:** Conceptualization; data curation; formal analysis; investigation; methodology; project administration; resources; validation; visualization; writing – original draft; writing – review and editing. **Kenzo Hokazono:** Conceptualization; data curation; formal analysis; investigation; methodology; project administration; resources; supervision; validation; visualization; writing – original draft; writing – review and editing.

FUNDING INFORMATION

The authors do not declare a specific grant for this research from any funding agency in the public, commercial, or not-for-profit sectors.

CONFLICT OF INTEREST STATEMENT

The authors declare that they have no competing interests.

DATA AVAILABILITY STATEMENT

The data substantiating this study have been incorporated within the article itself, and can be located in references 1 through 12.

ETHICS STATEMENT

The article describes a case report. Therefore, no additional permission from Ethics Committee was required.

CONSENT

Written informed consent was obtained from the patient to publish this report in accordance with the journal's patient consent policy.

ORCID

Paula Basso Dias  <https://orcid.org/0000-0002-3163-8854>

Anna Carolina Badotti Linhares  <https://orcid.org/0000-0001-5924-5078>

Kenzo Hokazono  <https://orcid.org/0000-0003-2897-6833>

REFERENCES

- Shields CL, Benevides R, Materin MA, Shields JA. Optical coherence tomography of retinal astrocytic hamartoma in 15 cases. *Ophthalmology*. 2006;113:1553-1557. doi:10.1016/j.ophtha.2006.03.032
- Krueger DA, Northrup H. Tuberous sclerosis complex surveillance and management: recommendations of the 2012 international tuberous sclerosis complex consensus conference. *Pediatr Neurol*. 2013;49:255-265.
- Aziria A, Chapron T, Martin G, Krystal S, Clement A, Caputo G. Tuberous sclerosis: diagnosis on ocular fundus examination. *J Fr Ophthalmol*. 2021;44:399-402. doi:10.1016/j.jfo.2020.10.010
- Zheng F, Deng X, Zhang Q, et al. Advances in swept-source optical coherence tomography and optical coherence tomography angiography. *Adv Ophthalmol Pract Res*. 2022;3:67-79.
- Pichi F, Massaro D, Serafino M, et al. Retinal astrocytic hamartoma: optical coherence tomography classification and correlation with tuberous sclerosis complex. *Retina*. 2016;36:1199-1208. doi:10.1097/IAE.0000000000000829
- Mutolo MG, Marciano S, Benassi F, Pardini M, Curatolo P, Emberti Gialloreti L. Optical coherence tomography and infrared images of astrocytic hamartomas not revealed by funduscopy in tuberous sclerosis complex. *Retina*. 2017;37:1383-1392.
- Hodgson N, Kinori M, Goldbaum MH, Robbins SL. Ophthalmic manifestations of tuberous sclerosis: a review: ocular findings in tuberous sclerosis. *Clin Exp Ophthalmol*. 2017;45:81-86.
- Rowley SA, O'Callaghan FJ, Osborne JP. Ophthalmic manifestations of tuberous sclerosis: a population based study. *Br J Ophthalmol*. 2001;85:420-423. doi:10.1136/bjo.85.4.420
- Zhang C, Xu K, Long Q, et al. Clinical features and optical coherence tomography findings of retinal astrocytic hamartomas in Chinese patients with tuberous sclerosis complex. *Graefes Arch Clin Exp Ophthalmol*. 2020;258(4):887-892. doi:10.1007/s00417-019-04476-y
- Kato A, Obana A, Gohto Y, Seto T, Sasano H. Optic coherence tomography appearances of retinal astrocytic hamartoma and systemic features in tuberous sclerosis of Japanese patients. *Eur J Ophthalmol*. 2019;29(3):330-337. doi:10.1177/1120672118787441
- Gao L, Wang FH, Chen N, Dong CX, Liu SJ. Non-symmetry in the calibre of retinal blood vessels. *Int J Ophthalmol*. 2009;9:1537-1539.
- Zhang ZQ, Shen C, Long Q, et al. Sirolimus for retinal astrocytic hamartoma associated with tuberous sclerosis complex. *Ophthalmology*. 2015;122:1947-1949.

How to cite this article: Dias PB, Linhares ACB, Hokazono K. Retinal hamartomas at different stages in a patient with tuberous sclerosis: A OCT-SS description. *Clin Case Rep*. 2023;11:e8185. doi:10.1002/ccr3.8185